

# Exhalative Mineralization in Devonian Reef Complexes of the Canning Basin, Western Australia

PHILLIP E. PLAYFORD<sup>†</sup>

*Geological Survey of Western Australia, East Perth, Western Australia 6004, Australia*

AND MALCOLM W. WALLACE

*School of Earth Science, University of Melbourne, Victoria 3010, Australia*

## Abstract

Lenticular stromatolite-barite-sulfide mounds, interpreted as sedimentary exhalative deposits, are exposed at several localities in Devonian reef complexes of the Canning basin, Western Australia. These mounds, hundreds of meters long and tens of meters thick, occur along contacts between basinal shales (Gogo Formation) and marginal-slope limestones (Sadler Limestone) and adjacent to synsedimentary faults cutting the Gogo Formation. The mounds are limestone buildups, composed of stromatolites intergrown with barite and cut by iron sulfide veins. The iron sulfides (marcasite and pyrite) are weathered to gossans at the surface. They fill fissures that probably formed as a result of contemporary seismic activity and the early compaction of underlying and adjoining shales. The stromatolite-barite-sulfide deposits also occur as allochthonous clasts in penecontemporaneous debris-flow deposits.

Postdepositional compaction of basinal shales in the Gogo Formation commonly amounted to about 75 percent. This resulted in the expulsion of large volumes of fluids along permeable interbeds, shale-limestone contacts, and synsedimentary faults, reaching the sea floor as cool-fluid seepages. The expelled fluids carried dissolved carbonate, barium, iron, and reduced sulfur. They probably nourished chemosynthetic bacteria that mediated the deposition of stromatolites, barite, and iron sulfides, resulting in growth of the stromatolite-barite-sulfide buildups.

There is no known economic mineralization in the exhalative buildups, but some drill holes encountered minor uneconomic veins of epigenetic Zn-Pb mineralization, filling narrow fissures that postdate the exhalative deposits. Economic epigenetic Zn-Pb deposits that have been mined elsewhere in the same general area of the Canning basin were formed during the early Carboniferous or latest Devonian, many millions of years after the exhalative deposits. Both exhalative and epigenetic phases of mineralization are thought to have been sourced through the compaction-driven dewatering of shales. The exhalative deposits are interpreted to have formed over seepages of cool fluids having salinities close to that of seawater, whereas the epigenetic deposits formed from much hotter fluids, probably brines, expelled during subsequent shale compaction.

## Introduction

THERE IS A consensus view that the economic Zn-Pb mineralization known in Devonian reef complexes of the Lennard shelf, in the Canning basin of Western Australia, is epigenetic (Ringrose, 1989; Murphy, 1990; McManus and Wallace, 1992; Tompkins et al., 1994a, b; Christensen et al., 1995; Vearncombe et al., 1995). However, an earlier phase of syngenetic mineralization, associated with stromatolite buildups, has recently been recorded in the same general area and is interpreted to have formed as mounds over cool-fluid seepages on the sea floor (De Keever, 1998; Mason, 1998; Playford and Wallace, 1998; Playford, 1999; Playford et al., 1999).

Although there is general agreement that the economic Zn-Pb mineralization in the Canning basin is epigenetic, there is no similar consensus regarding many Zn-Pb deposits known elsewhere in Australia and the world. For example, Large et al. (1998) and Cooke et al. (2000) have presented evidence that the Mount Isa and McArthur River deposits in northern Australia are sedimentary-exhalative deposits, whereas Perkins and Bell (1998) have interpreted the same deposits as epigenetic, and Broadbent et al. (1998) maintain that the

comparable Century deposit is also epigenetic. Likewise, several authors have interpreted the Irish Zn-Pb orebodies as sedimentary-exhalative deposits (e.g., Boyce et al., 1983; Banks, 1985; Russell, 1996), whereas others have claimed that the same deposits are epigenetic (e.g., Shearley et al., 1996; Hitzman and Beaty, 1997; Peace and Wallace, 2000).

In view of this international controversy regarding syngenetic vs. epigenetic origins of many Zn-Pb deposits, it is important to examine evidence for the reported occurrence of syngenetic (exhalative) mineralization in Devonian carbonates of the Canning basin and to compare and contrast it to known epigenetic mineralization in the same general area.

## Devonian Reef Complexes of the Canning Basin

Devonian reef complexes are well exposed on the Lennard shelf, the northernmost structural subdivision of the Canning basin, forming a series of limestone ranges some 350 km long (Fig. 1). The reef complexes were constructed as shallow reef-fringed limestone platforms, fronted by steeply dipping marginal-slope deposits, which descended into flat-lying basin deposits in water up to several hundred meters deep (Playford, 1980; Kerans, 1985; Wallace et al., 1991; Playford and Cockbain, 1992; Vearncombe et al., 1995; Playford and Hocking, 1999; Copp, 2000).

<sup>†</sup> Corresponding author: e-mail, p.playford@dme.wa.gov.au

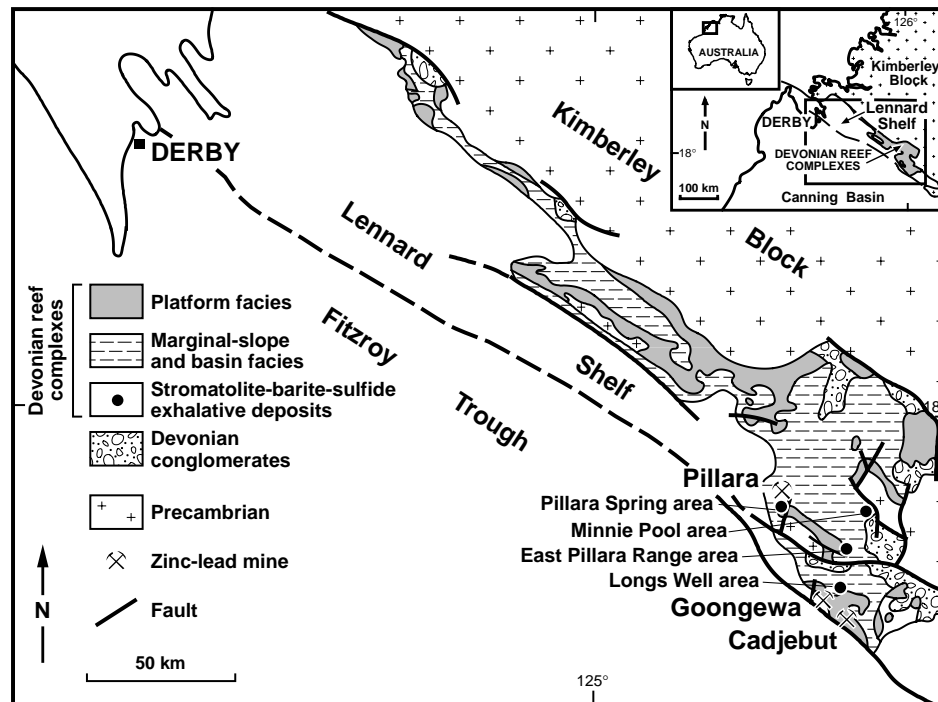


FIG. 1. Locality map and generalized geologic map of Devonian reef complexes of the Canning basin, showing the locations of exhalative deposits and principal Zn-Pb mines.

Mounds of distinctive stromatolitic limestone, commonly intergrown with barite and cut by gossan veins, are exposed at several localities in basin facies of the Gogo Formation in the southeastern Lennard shelf (Figs. 1, 2). The descriptive term “buildup” is used here to describe these mounds, rather than the genetic term “bioherm,” because both organic and inorganic precipitation may have been involved in their growth.

The stromatolite-barite-gossan deposits are exposed in four main areas of the northern Canning basin, in the southeastern Lennard shelf (Figs. 1, 3). They are developed (1) where the basin facies of the Gogo Formation adjoins marginal-slope facies of the Sadler Limestone (Fig. 4), (2) at other places where the Gogo Formation is cut by syndimentary faults, and (3) as allochthonous clasts in penecontemporaneous debris-flow conglomerates that intertongue with the Gogo Formation.

The stromatolitic buildups in each of these areas are cut by limonitic gossan veins, most of which are near vertical and approximately parallel or perpendicular to the trend of each buildup. Others developed where fissures opened along bulbous bedding. Drilling has shown that the gossans have formed by the weathering of iron sulfides (pyrite and marcasite). Neomorphic alteration adjacent to the gossans has resulted in recrystallization of the stromatolitic limestones to dark fibrous calcite, with partial destruction of their original stromatolitic fabrics.

The major part of the Gogo Formation consists of shale and siltstone, containing many limestone concretions (Gogo concretions) in places where the formation adjoins the Sadler Limestone and especially where stromatolitic buildups are developed (Fig. 5).

Economic Zn-Pb deposits (Mississippi-Valley-type deposits) have been found in the same general area of the Lennard shelf but not in the specific localities where the stromatolite-barite-sulfide deposits occur (Fig. 1). The Zn-Pb deposits formed where mineralizing fluids were channeled along faults and joints and through hydrothermal caverns in the Devonian carbonates. McManus and Wallace (1992) deduced on petrographic grounds that the epigenetic Zn-Pb mineralization occurred during the latest Devonian (late Famennian) or early Carboniferous. Their interpretation was confirmed using Rb-Sr and U-Pb isotope techniques by Christensen et al. (1995), who dated the Zn-Pb mineralization as  $357 \pm 3$  Ma, and Brannon et al. (1996), who dated it as  $351 \pm 15$  Ma. Those dates would place the mineralization in the latest Devonian to earliest Carboniferous according to Young and Laurie (1996) or the early Carboniferous according to Tucker et al. (1998). Christensen et al. (1995) further concluded that the mineralizing fluids were derived by dewatering of Devonian shales and speculated that exhalative mineralization, equivalent in age to the epigenetic deposits, might occur in the uppermost Devonian and lower Carboniferous Fairfield Group, which overlies the reef complexes.

The exhalative deposits have not been dated by radiometric methods, but equivalent strata in the youngest Gogo Formation have been dated by conodonts as early Frasnian (about 365–380 Ma), within Frasnian conodont zone 5 (Gilbert Klapper, writ. commun., 1998, 1999).

#### Field Relationships

The four principal areas where stromatolite-barite-gossan (sulfide) deposits are exposed are referred to as the Longs

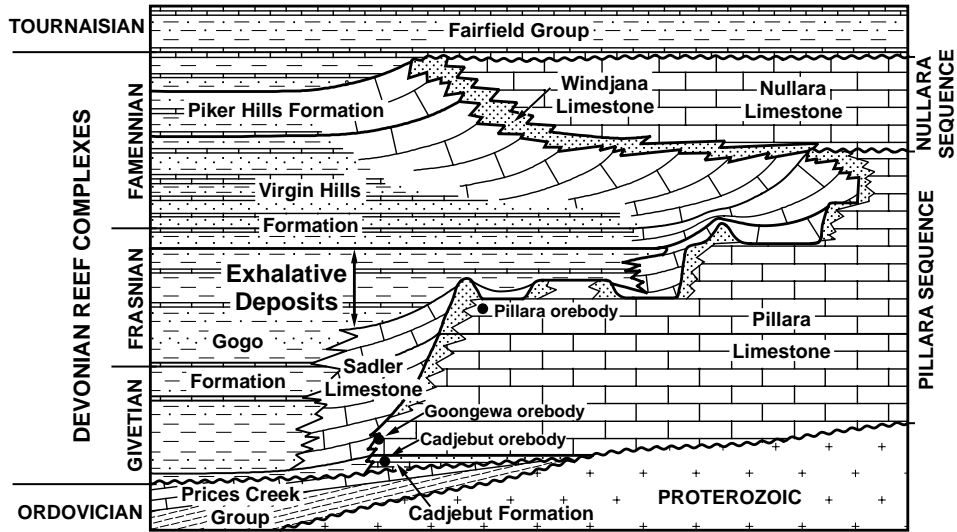


FIG. 2. Diagrammatic section showing subdivisions of the Devonian reef complexes and the stratigraphic positions of the exhalative deposits and principal epigenetic Zn-Pb orebodies.

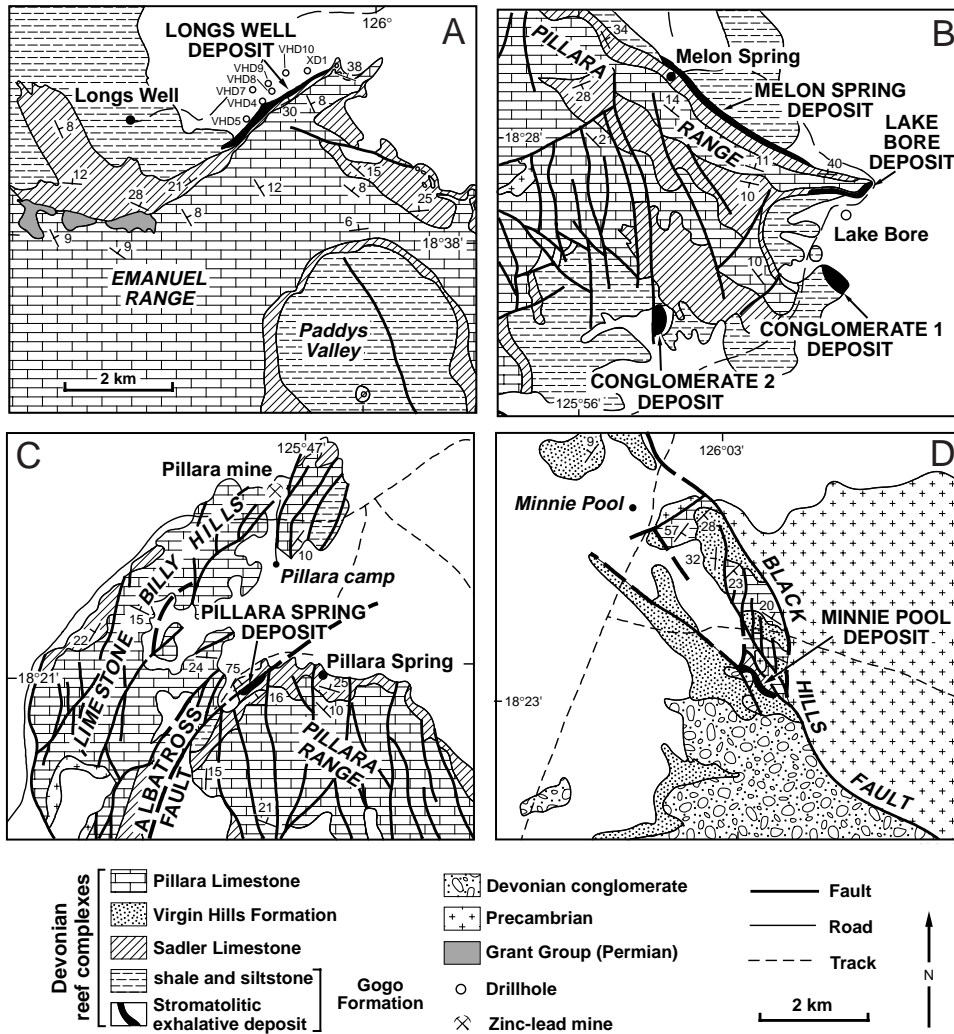


FIG. 3. Geologic maps showing the locations of stromatolite-barite-sulfide exhalative deposits. A. Longs Well deposit. B. East Pillara Range deposits. C. Pillara Spring deposit. D. Minnie Pool deposit. Geology modified from Playford and Hocking (1999).

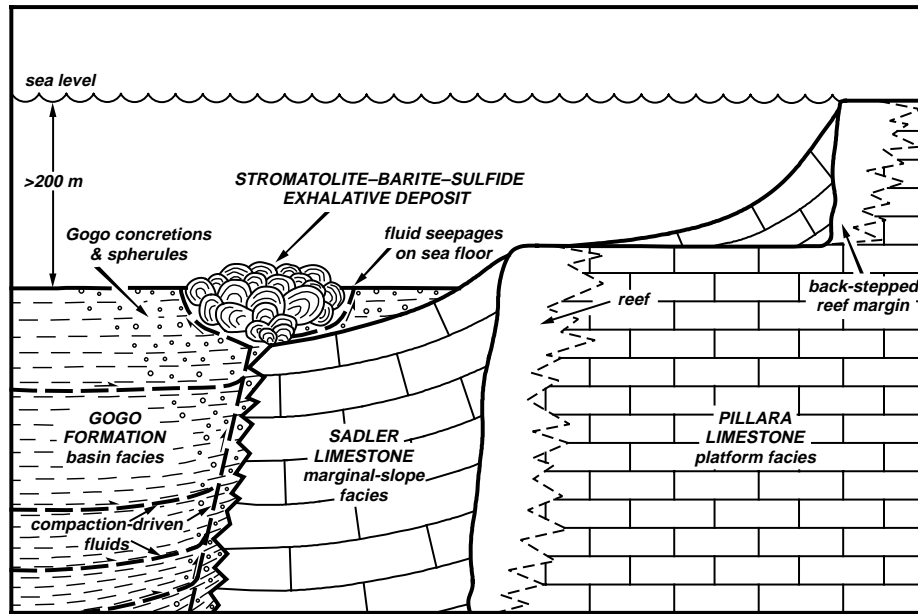


FIG. 4. Diagrammatic section illustrating the development of stromatolite-barite-sulfide exhalative deposits in the Gogo Formation, associated with backstepping of platform deposits in the Pillara Limestone. Modified from Playford (1999).

Well, East Pillara Range, Pillara Spring, and Minnie Pool areas (Fig. 3).

#### Longs Well area

A belt of stromatolitic limestone, intergrown with barite and cut by prominent gossan veins, forms a linear buildup, 2.6 km long, 150 m wide, and at least 50 m thick, along the north side of the Emanuel Range near Longs Well (Fig. 3A, Fleming, 1983; Bennett, 1992, 1994; De Kever, 1998). The buildup occurs within the Gogo Formation, adjoining the contact with the Sadler Limestone.

The buildup formed as a coalesced series of bulbous stromatolitic growths (Figs. 4–8). Most barite was deposited

contemporaneously with the stromatolites, as fibrous or bladed crystals and rosettes and unidirectional dendritic forms intergrown with stromatolites, but some fills narrow fissures cutting the stromatolites and intergrown barite (Figs. 6, 9).

The stromatolitic buildup is cut by many black, brown, and red gossan veins, occupying fissures up to 5 m wide and a few tens of meters long (Figs. 5, 6, 9), and surrounded by zones of dark, fibrous, recrystallized calcite (Fig. 7G-H). Drill holes show that the gossans originated through the weathering of pyrite and marcasite. In a few places, gossanous material fills spaces between stromatolite columns (Figs. 6, 9C), and some gossan veins exhibit stromatolite-like layering.

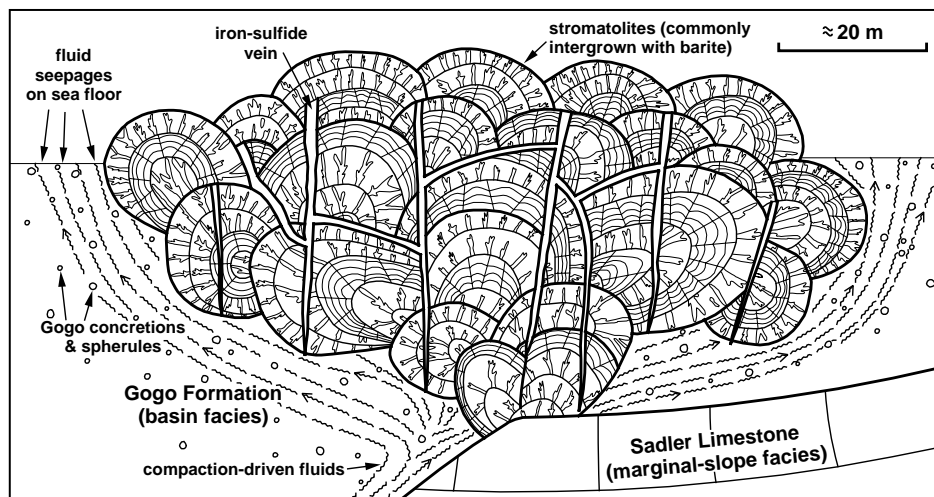


FIG. 5. Diagrammatic section illustrating the development and morphology of stromatolite-barite-sulfide exhalative deposits, with associated concretions and spherules, formed over compaction-driven cool-water seepages.

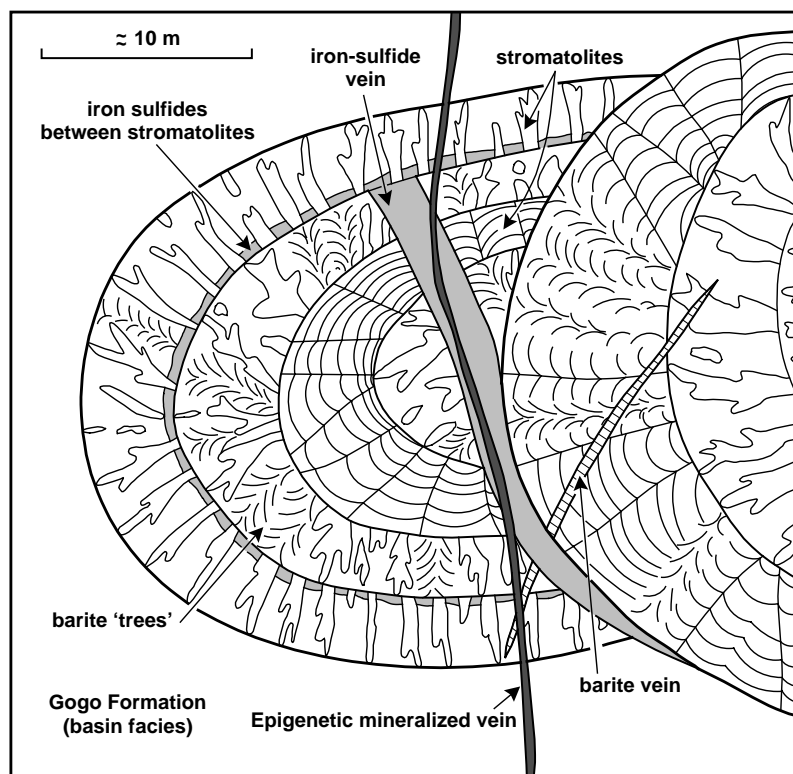


FIG. 6. Diagrammatic section illustrating relationships between stromatolites, barite, and iron sulfides in the exhalative deposits and subsequent epigenetic mineralization.

#### *East Pillara Range area*

Four stromatolite-barite-gossan deposits, referred to as the Melon Spring, Lake Bore, Conglomerate 1, and Conglomerate 2 deposits, occur in the vicinity of the East Pillara Range (Fig. 3B).

The Melon Spring and Lake Bore deposits resemble the Longs Well deposit but are less well exposed. Some gossans in the Lake Bore deposit display well-defined stromatolitic structures (Fig. 9B).

In the Conglomerate 1 and Conglomerate 2 deposits the stromatolite-barite-gossan association is represented by large allochthonous clasts in debris-flow conglomerates that inter-tongue with the Gogo Formation. These conglomerates contain rounded boulders and cobbles of Precambrian quartzite, together with angular blocks of stromatolitic limestone (up to 18 m long), smaller blocks of gossan and barite, reworked Gogo concretions (Fig. 8E), and some clasts of marginal-slope and platform limestones. The Conglomerate 1 deposit also displays some remarkable circular stromatolitic bodies, thought to have grown as spheres below the surface of muds in the Gogo Formation (Fig. 7F).

Many blocks of stromatolitic limestones in the conglomerates are wholly or partly recrystallized, although the bulbous stromatolitic layering has commonly been maintained. Recrystallization is thought to have predated incorporation of the stromatolitic blocks in the conglomerate. Debris flows must have been swept into the basin, breaking up stromatolite-barite-sulfide buildups that were then growing on the basin floor.

#### *Pillara Spring area*

The Pillara Spring deposit (Fig. 3C) is a discontinuous belt of stromatolitic limestone between the Pillara Range and Limestone Billy Hills reef complexes, adjoining the Albatross fault, a northeast-trending synsedimentary normal fault having a left-lateral component of movement (Dörfling et al., 1995). The limestone consists of contiguous columns of fibrous stromatolites, partly recrystallized and cut by a few prominent gossans, but no barite has been observed. Gogo concretions and spherules are abundant in steeply dipping Gogo Formation on the northwest side of the fault (Fig. 8F).

#### *Minnie Pool area*

The Minnie Pool deposit consists of stromatolites intergrown with barite and cut by veins of gossan and barite. The deposit adjoins the Sadler Limestone and underlies the Virgin Hills Formation, forming low outcrops within a strongly faulted zone (Fig. 3D). Stromatolites are well preserved in some exposures (Fig. 7A) but have been largely destroyed through recrystallization in others, especially where the limestone adjoins gossans. There is evidence, in the form of penecontemporaneous neptunian dikes (Playford, 1980) containing fragments of barite and Devonian limestones, that the faulting was synsedimentary.

#### **Stromatolite Buildups**

In view of the different ways in which the term "stromatolite" has been applied by various authors, it is necessary to clarify the usage adopted in the present paper. We adopt a

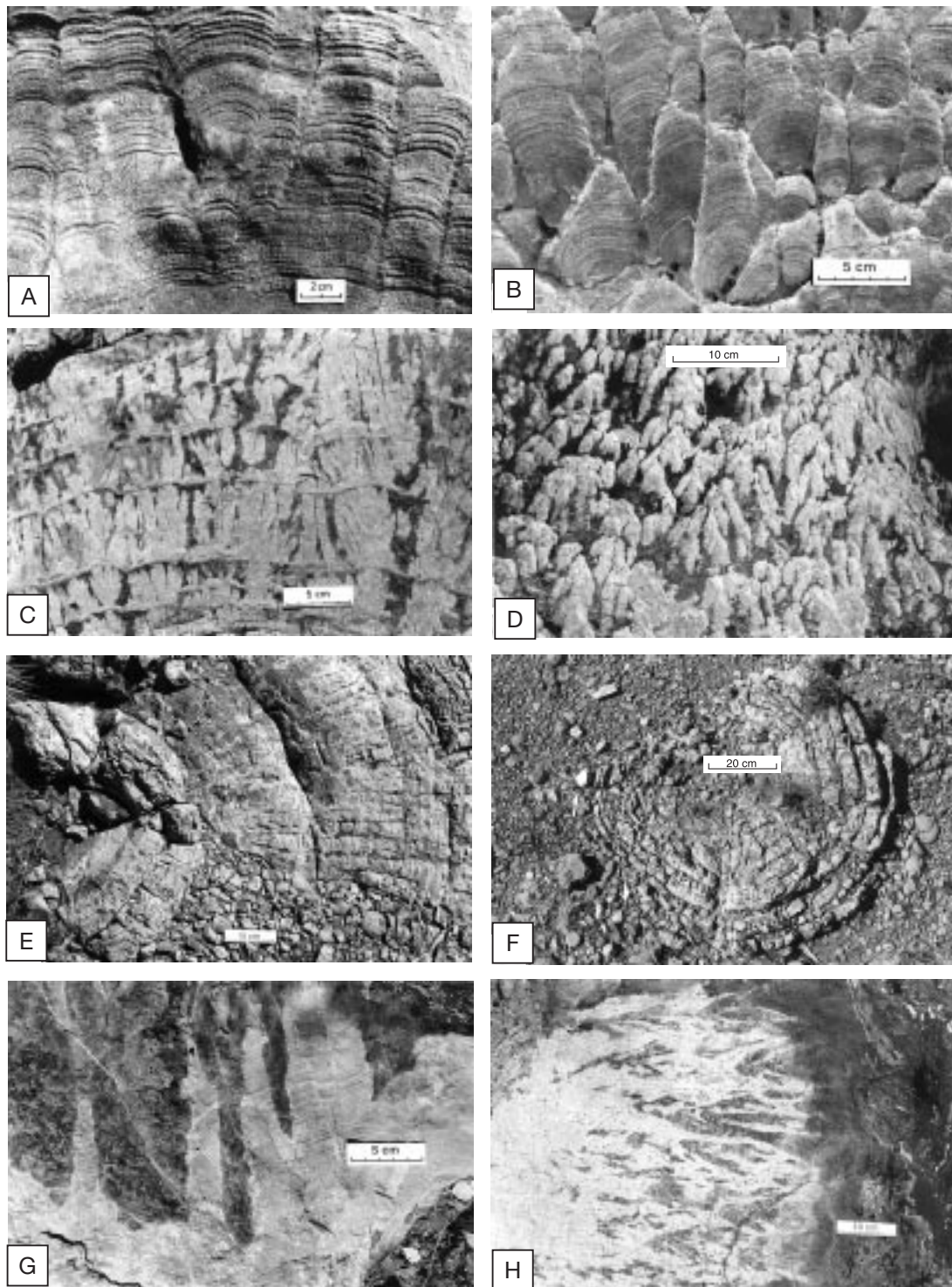


FIG. 7. Stromatolites. A. Contiguous columnar fibrous-micritic stromatolites, Minnie Pool deposit. B. Contiguous columnar stromatolites, Longs Well deposit. C. Successive layers of digitate stromatolites, Conglomerate 2 deposit. D. Digitate stromatolites that grew downward from the base of a bulbous stromatolite body, Longs Well deposit. E. Bulbous stromatolite body constructed by columnar stromatolites, Conglomerate 2 deposit. F. Circular cross section through a stromatolite body, probably originally spherical in shape, Conglomerate 1 deposit. G. Dark-colored recrystallized stromatolitic limestone (upper part), replacing light-colored stromatolitic limestone, with an abrupt interfingering contact between them, Longs Well deposit. H. Black gossan (on the extreme right) cutting through dark-colored recrystallized limestone, passing (in the center) into partly recrystallized stromatolitic limestone, then into light-colored (unaltered) stromatolitic limestone, Longs Well deposit.

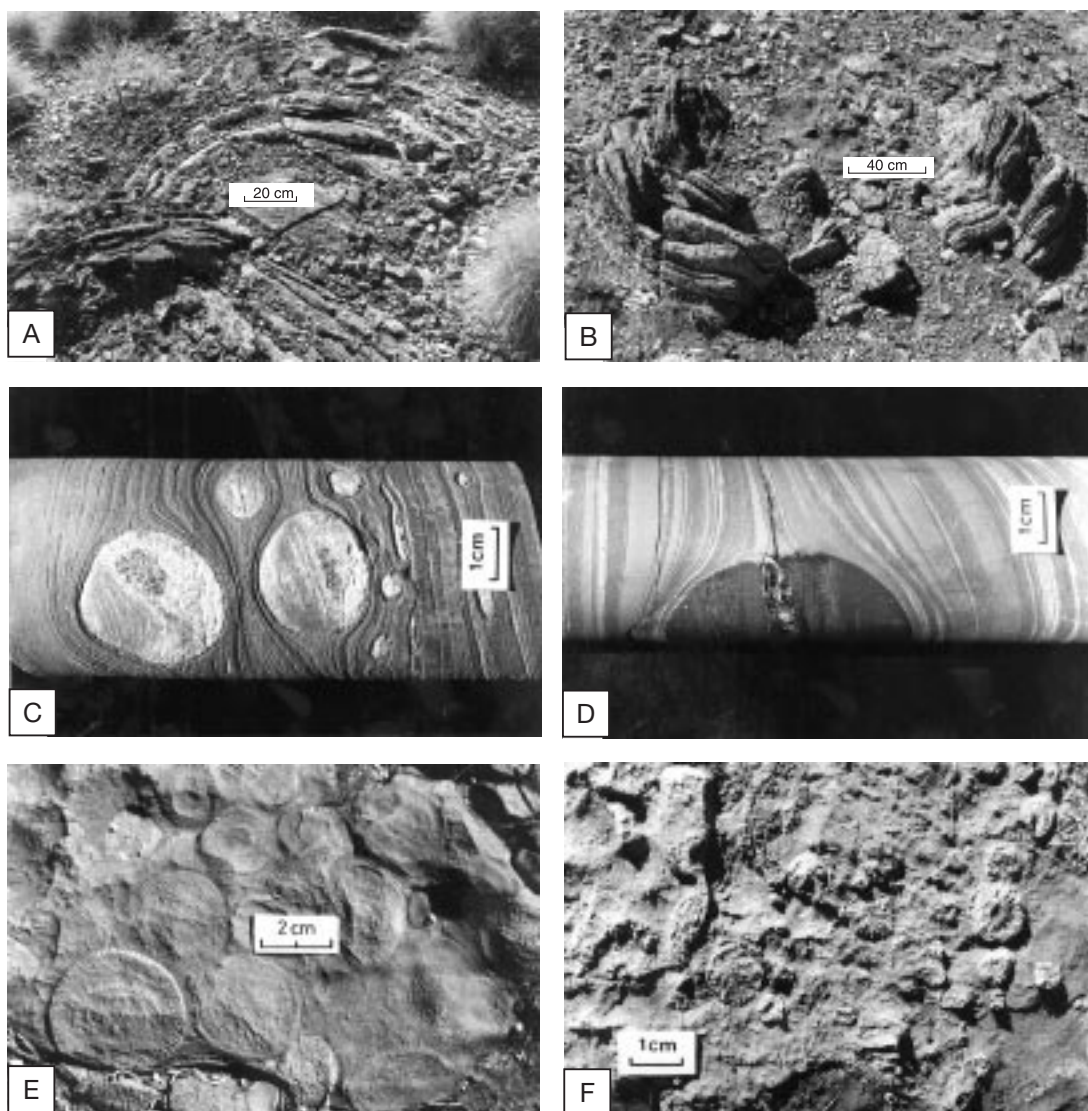


FIG. 8. Stromatolites, Gogo concretions, and spherules. A. Successive bulbous stromatolite growths, Conglomerate 1 deposit. B. Bulbous stromatolite body, forming a large allochthonous block, Conglomerate 1 deposit. C. Drill core showing Gogo concretions and compaction of adjoining shale in the Gogo Formation, Limestone Billy Hills area. D. Drill core showing a Gogo concretion formed around an ammonoid and strong compaction of equivalent shale in the Gogo Formation, Limestone Billy Hills area. E. Gogo concretions showing outer layers of fibrous calcite, Conglomerate 1 deposit. F. Fibrous calcite spherules, Pillara Spring deposit.

broad usage of the term, defining stromatolites as “columnar, digitate, and domal growth structures formed by organic or inorganic processes.” This does not comply with some various restricted definitions that require stromatolites to be organic (e.g., Walter, 1976) and laminated (e.g., Riding, 2000).

A variety of both shallow- and deep-water stromatolites has been recorded from the Devonian reef complexes of the Canning basin, but the forms described in the present paper differ from those previously recorded by Playford et al. (1976). Whereas the previously known stromatolites formed on shallow reefal platforms and down fore-reef slopes and were associated with open-marine benthic faunas, the stromatolites discussed here grew on the floors of deep inter-reef basins, surrounded by anoxic muds and without associated benthic

faunas (Figs. 4, 5). Most of the present forms, unlike those previously described, are composed of radiating fans of fibrous calcite, commonly interspersed with micritic laminae. Gradations are found between columns composed entirely of calcite fibers and those consisting largely of laminated micrite. The fibrous calcite forms radiating fans, generally having radii of around 10 to 20 mm (Fig. 7A).

In outcrop, the fibrous calcite has two forms: white to light gray calcite (here termed light-colored calcite) and dark brown to black calcite (here termed dark-colored calcite). Stromatolitic fabrics are well preserved in light-colored calcite but are largely destroyed through recrystallization in the dark-colored form. Inclusions are very abundant in light-colored calcite and rare in dark-colored calcite. Most inclusions in the

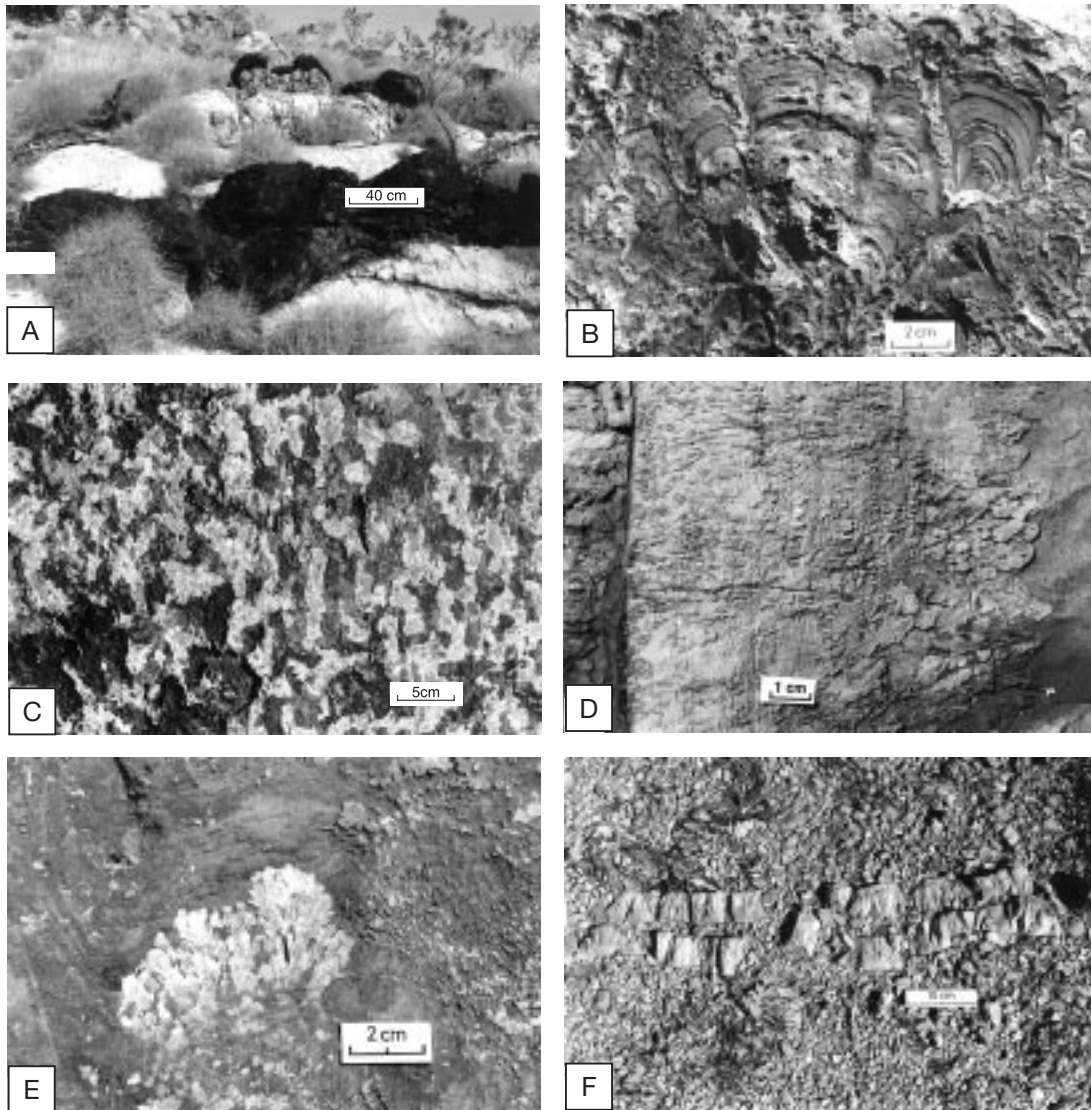


FIG. 9. Gossans and barite. A. Gossan veins cutting through stromatolitic limestone, Longs Well deposit. B. Stromatolites in gossan, Lake Bore deposit. C. Black gossan filling spaces between stromatolite columns, Longs Well area. D. Finely dendritic barite, intergrown with stromatolitic limestone, with more massive dendritic barite on the left, Longs Well deposit. E. Barite shrub and bladed dendritic crystals intergrown with stromatolitic limestone, Longs Well deposit. F. Narrow barite vein cutting through dendritic barite, Minnie Pool deposit.

light-colored calcites are subspherical and opaque to translucent and are probably composed of organic material. The fluid inclusions are less common and are mostly small (less than 10  $\mu\text{m}$ ) and single phase, indicating that the calcite was precipitated at relatively low temperatures, less than 60°C (Goldstein and Reynolds, 1994).

The dark-colored calcite is clearly a recrystallization product of the light-colored form, as it cuts across primary stromatolitic fabrics (Fig. 7G-H). Patches of recrystallized dark-colored calcite are commonly dispersed through the unaltered light-colored form and vice versa, generally with sharp boundaries between them. Sparse pyrite inclusions, less than 10  $\mu\text{m}$  in diameter, are present in subsurface samples of dark-colored calcite but are absent from the light-colored

form. The pyrite inclusions weather to iron oxide at the surface.

The dark-colored limestone occurs in zones, ranging from less than a meter to several meters wide, mostly adjoining gossan veins. Dark-colored calcite has uniform stable isotope compositions, with  $\delta^{18}\text{O}$  and  $\delta^{13}\text{C}$  values ranging from -7 to -5 and -22 to -19 per mil PDB, respectively. Light-colored calcite is much more variable, with  $\delta^{18}\text{O}$  and  $\delta^{13}\text{C}$  values ranging from -12 to -6 and -20 to -7 per mil PDB, respectively (De Kever, 1988; Mason, 1998). Relative to marine carbonates, both types of fibrous calcite have very negative carbon isotope signatures, with dark-colored calcite having lower  $\delta^{13}\text{C}$  and higher  $\delta^{18}\text{O}$  values than the light-colored type (Fig. 10).

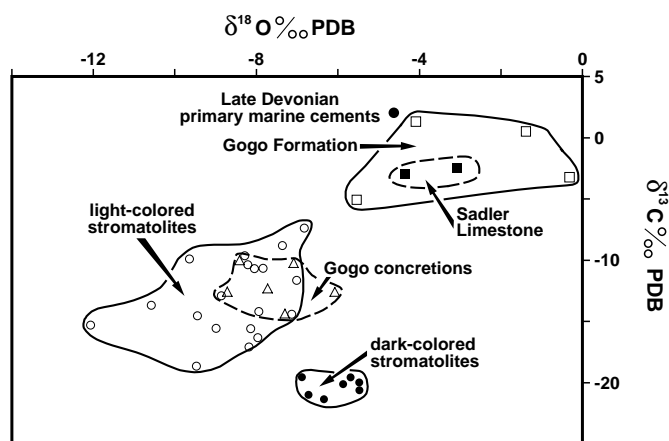


FIG. 10. Diagram illustrating oxygen and carbon isotope values for stromatolites, Gogo concretions, Sadler Limestone, Gogo Formation, and Late Devonian primary marine cements. Analytical data from De Keever (1998) and Mason (1998).

Trace element compositions of light-colored calcite are quite distinct from those of dark-colored calcite (De Keever, 1998; Mason, 1998). Dark-colored calcite has higher concentrations of magnesium, strontium, and manganese (magnesium values 1.2–2.1 wt %, strontium 400–1200 ppm, and manganese 0.4–1.2 wt %) than light-colored calcite (magnesium 0–0.8 wt %, strontium 0–800 ppm, and manganese 0–1.1 wt %). Dark-colored calcite generally has lower concentrations of iron (0–1,000 ppm) than light-colored calcite (0–3,000 ppm; Fig. 11).

The stromatolitic buildups formed where the upper Gogo Formation overlapped the Sadler Limestone, associated with periods of abrupt backstepping of the platforms in the early Frasnian (Fig. 4). Deposition in the basin was very slow at those times, as little reef-derived debris was able to reach the basins. The buildups generally began growth directly on Sadler Limestone, developing as bulbous outgrowths, about 5 to 40 m across, which coalesced to form lenticular buildups as much as 3.5 km long, 150 m wide, and 50 m thick. Each bulbous outgrowth consists of successive layers of spaced, contiguous, and branching columnar stromatolites (Figs. 4–8).

Unlike the stromatolites described by Playford et al (1976), which commonly grew vertically, toward light or under the influence of gravity, individual stromatolites in these buildups grew radially outward, at right angles to the bulbous layering. Thus, a bulbous outgrowth can include stromatolites that grew downward at the base, horizontally on the sides, and upward on top. Chemosynthetic bacteria probably played significant roles in carbonate precipitation and associated barite and sulfide mineralization, although this has not been proved, as no cellular or filamentous structures have been identified.

Field and petrographic evidence, in the form of sediment draped over stromatolites, suggests that the upper parts of the buildups grew as low mounds on the sea floor. However, the lower parts of the buildups may have grown into muds below the surface. Certainly the stromatolites at the base of some bulbous bodies grew downward (Fig. 7D), but it has not been proven whether they grew into mud or water. On the other hand, it is clear that the fibrous rims on Gogo concretions (described below, see Fig. 8E) grew totally enclosed in mud, and the fibers in those concretions have the same characteristics as those of fibrous stromatolites.

### Gogo Concretions

A characteristic feature of the Gogo Formation in the vicinity of the stromatolitic buildups is the presence of abundant spherical to ovoid limestone concretions, commonly 5 to 20 cm in diameter (Fig. 5), which commonly weather out at the surface in large numbers. In some cases, the outer layers of the concretions consist of radial fibrous calcite (Fig. 8E), which must have grown by displacement of the surrounding mud. Masses of small spherules, about 2 to 15 mm in diameter, are associated with concretions and stromatolitic buildups in some areas (Fig. 8F). They consist of radial calcite fibers, of the same type as those that surround some Gogo concretions.

The concretionary calcite has  $\delta^{18}\text{O}$  and  $\delta^{13}\text{C}$  values ranging from  $-8.4$  to  $-6.0$ – $-14.5$  to  $-10$  per mil PDB, respectively, values that are similar to those for light-colored fibrous stromatolites (Fig. 10). The trace element content of concretionary fibrous calcite is also similar, with magnesium ranging from 0.04 to 0.25 wt percent; strontium from 0 to 700 ppm, manganese

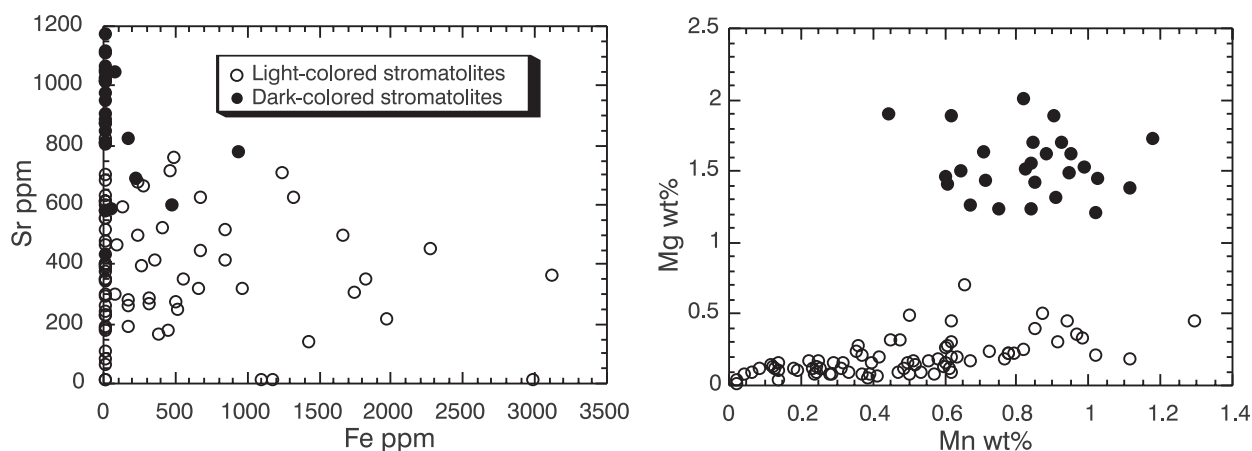


FIG. 11. Diagram illustrating iron, manganese, magnesium, and strontium contents of light- and dark-colored stromatolites. Analytical data from De Keever (1998) and Mason (1998).

from 0 to 0.6 wt percent, and iron from 0 to 600 ppm (De Keever, 1998; Mason, 1998).

Relatively thick lamination is preserved in the concretions, and this can be traced into very fine lamination in the adjoining compacted shales (Fig. 8C-D). Measurements of bedding thicknesses in concretions and equivalent laminae in shales show that postdepositional compaction was commonly as much as 75 percent. This compaction must have resulted in the expulsion of large volumes of intrastratal water and gas.

### Barite Mineralization

Barite is widespread in most stromatolitic buildups, mainly in the form of dendritic growths and shrubs of fibrous barite, which form layers up to 2 m thick, intergrown with stromatolites (Figs. 6, 9D-E). The dendritic barite resembles "plumose barite" described by Kaiser et al. (1987), and its interrelationships with calcite indicate that the two minerals were coprecipitated. Barite also occurs as veins (Fig. 9F), generally less than a meter wide, cutting through slightly older barite and stromatolites, and as small rosettes and randomly oriented blades replacing calcite. Analyses show barium contents ranging from 32.01 percent in dendritic barite to 53.96 percent in a barite vein. The total barite content of buildups ranges from an estimated 5 to 10 percent in the Minnie Pool and Longs Well deposits to nil in the Pillara Spring deposit.

Barite has  $\delta^{34}\text{S}$  values ranging from 38 to 50 per mil CDT (Fig. 12). These values are consistent with derivation of the mineralizing fluids from residual sulfur remaining after extensive sulfate reduction in a closed system. The sulfur isotope composition in the barite is not consistent with marine fluids, as marine sulfates are characterized by lower  $\delta^{34}\text{S}$  values (Claypool et al., 1980). The isotopic composition of the barite also suggests that evaporites in the Cadjebut Formation (Hocking et al., 1996), which have  $\delta^{34}\text{S}$  values of about 20 per mil CDT (Tompkins et al., 1994b), did not constitute a source of sulfate for the deposits.

Sulfur isotopes enriched in  $\delta^{34}\text{S}$  have been recorded where bacterial sulfate reduction is taking place in pore waters of modern sediments (Masuzawa et al., 1992). Moreover, barium is commonly present in relatively high concentrations (250–800 ppm) in shales, either as barite or combined with organic matter (Paytan et al., 1993). In either case, barium can be mobilized readily in the zone of sulfate reduction (Goldberg and Arrhenius, 1958; Torres et al., 1996; Church,

1979). It seems clear that the barium must have been derived from shales in the Gogo Formation and transported by fluids generated during early diagenesis.

### Gossans and Iron Sulfide Mineralization

One of the most conspicuous features of the outcropping stromatolitic buildups is the presence of black, brown, and red gossan veins, commonly up to several meters wide and tens of meters long, cutting through the buildups (Figs. 5, 6, 9A). Drill holes show that these limonitic gossans are weathering products of pyrite and marcasite.

The gossan veins fill fissures that opened up periodically during growth of the stromatolitic buildups, probably as a result of seismic activity and the early compaction of muds adjoining and underlying the buildups. Most fissures are sub-vertical or follow the bulbous bedding of major stromatolitic outgrowths (Fig. 5).

Some gossans display evidence of probable microbial involvement in growth of the precursor iron sulfides, in the form of well-preserved columnar stromatolites (Fig. 9B). Others exhibit stromatolite-like wavy lamination, which may have formed as a result of microbial processes, although an inorganic origin cannot be ruled out. However, most gossans are amorphous.

At a few localities, small amounts of gossanous material fill the interareas between stromatolite columns, indicating that iron sulfides were periodically precipitated over stromatolite growth surfaces (Figs. 6, 9C). This demonstrates the syngenetic origin of the sulfides, as does the occurrence of gossan clasts in penecontemporaneous debris-flow deposits in the Conglomerate 1 and 2 deposits.

Sulfur isotopes in the syngenetic pyrite and marcasite have very positive  $\delta^{34}\text{S}$  values, ranging from 33 to 37.5 per mil CDT, although they are less than the extremely high values for syngenetic barite (38–50‰ CDT; Fig. 12). Electron microprobe analyses indicate that the iron sulfides contain measurable concentrations of zinc, ranging from 2,080 to 730 ppm, and this metal is thought to be bound into the crystal lattice of the pyrite and marcasite—no sphalerite has been detected, other than in epigenetic Zn-Pb veins. Anomalously high zinc values (up to 7,410 ppm, see Table 1) have been recorded from some gossans, perhaps derived from zinc bound into the crystal lattice of the original iron sulfides. Lead values are generally very low in the iron sulfides but one sample contained 2,040 ppm of Pb (Table 1).

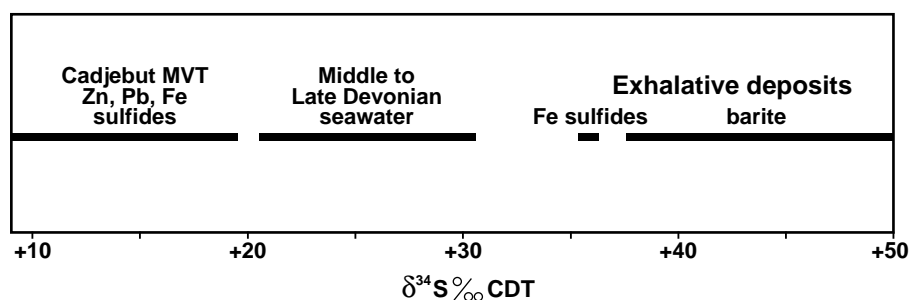


FIG. 12. Diagram illustrating sulfur isotope values for Cadjebut epigenetic Zn-Pb mineralization, Middle to Late Devonian seawater, and Late Devonian exhalative sulfides and barite. Some analytical data from Claypool et al. (1980), Tompkins et al. (1994b), De Keever (1998), and Mason (1998).

TABLE 1. Analytical Data from Surface Samples of Gossans and Drill Core Samples of Iron Sulfides in Stromatolite-Barite-Sulfide Exhalative Deposits

Deposit	Sample no.	Zn (ppm)	Pb (ppm)	Cu (ppm)	Ba (ppm)
Longs Well	134931	121	41	4	269
Longs Well	134954	104	46	10	322
Longs Well	134956	1,308	204	13	356
Longs Well <sup>1</sup>	V4-31-1	2,140	n.d.	n.d.	n.d.
Longs Well <sup>1</sup>	V4-31-2	1,560	n.d.	n.d.	n.d.
Conglomerate 1	134946	3	42	17	86
Conglomerate 1 <sup>1</sup>	ED35-107-1	940	n.d.	n.d.	n.d.
Conglomerate 1 <sup>1</sup>	ED35-107-2	2,080	n.d.	n.d.	n.d.
Conglomerate 1 <sup>1</sup>	ED35-107-3	1,770	2,040	n.d.	n.d.
Conglomerate 1 <sup>1</sup>	ED35-107-4	730	n.d.	n.d.	n.d.
Conglomerate 2	134952	7,410	131	49	87
Lake Bore	134949B	1,745	80	350	46
Lake Bore	134949C	222	118	84	29
Melon Spring	134950A	4,850	84	20	638
Melon Spring	134950B	2,282	56	9	250
Pillara Spring	134958	259	24	6	256
Pillara Spring	134961	716	38	9	695

<sup>1</sup> Drill core samples, data from De Keever (1998) and Mason (1998)

### Epigenetic Mineralization

Epigenetic mineralization, in the form of galena, sphalerite, and iron sulfides, occurs to a very minor extent in drill hole cores in the stromatolitic buildups, filling fissures up to a few centimeters wide, and as replacements of exhalative iron sulfides. These epigenetic Zn-Pb sulfides are more coarsely crystalline than the exhalative sulfides.

Where the epigenetic Zn-Pb sulfides fill, or partly fill, primary porosity, they postdate early nonluminescent calcite and regional dolomite but are older than dull luminescent calcite cements. They are also coeval with saddle dolomite, inclusion-rich calcite, and bright luminescent calcite cements (Fig. 13). These paragenetic relationships are consistent with those reported by McManus and Wallace (1992) in their study of the regional timing of epigenetic Zn-Pb mineralization on the Lennard shelf. Based on the radiometric dating of sphalerite

from Pillara and ore-stage calcite from Goongewa, Christensen et al. (1995) and Brannon et al. (1996) have since shown that the Zn-Pb mineralization occurred about 351 to 357 m.y. ago, during the latest Devonian or early Carboniferous. That dating is many millions of years later than growth of the stromatolitic buildups and their associated synsedimentary (exhalative) mineralization (about 10–16 m.y. later according to the timescale of Young and Laurie, 1996; or 22–28 m.y. later according to that of Tucker et al., 1998). It is estimated that during the episode of epigenetic mineralization the exhalative deposits would have been buried below more than 1,000 m of Upper Devonian sediments.

The Zn-Pb sulfides previously documented from the Cadjebut deposit have  $\delta^{34}\text{S}$  values ranging from 15 to 20 per mil CDT (Tompkins et al. 1994b), which are somewhat lower than those for Middle Devonian Cadjebut Formation evaporites (about 20‰ CDT), and much lower than for the exhalative

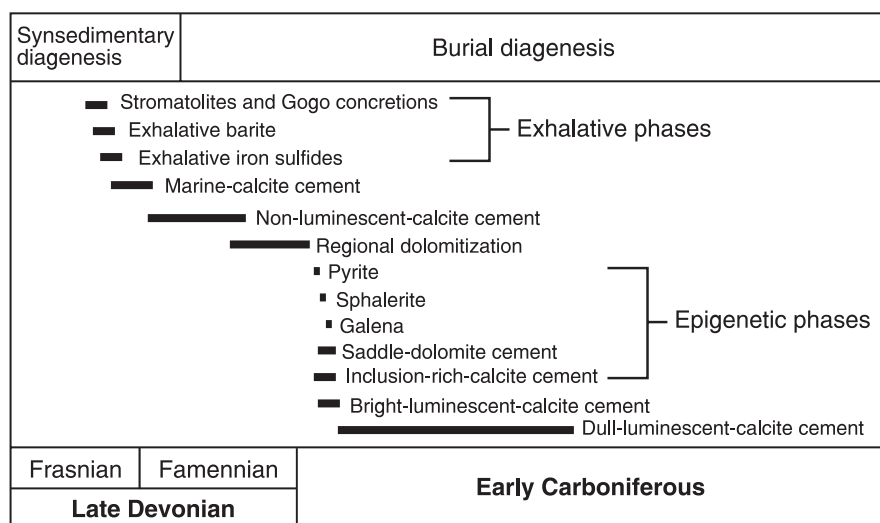


FIG. 13. Paragenetic sequences of exhalative phases, calcite cements, and epigenetic phases. Analytical data from De Keever (1998) and Mason (1998).

iron sulfides and barite described in this paper (33–37.5 and 38–50‰ CDT, respectively).

### Genesis of the Deposits

The stromatolite-barite-sulfide deposits are interpreted to have formed by precipitation over sea-floor seepages of cool fluids exhaled as a result of the compaction of basal shales in the Gogo Formation.

#### Source of mineralizing fluids

The major chemical processes involved in forming the mineralizing fluids are thought to have been organic matter oxidation and sulfate reduction during early diagenesis of shales in the Gogo Formation. Such reactions in organic-rich sediments are relatively well understood and include (from earliest to latest): bacterial oxidation of organic matter, bacterial sulfate reduction, and bacterial fermentation (methanogenesis; Curtis et al., 1972; Irwin et al., 1977). Such reactions liberate bicarbonate to the pore waters and produce  $\delta^{13}\text{C}$ -depleted fluids, together with reduced sulfur.

The calcite in stromatolites of the exhalative buildups is characterized by very negative carbon isotopes, with  $\delta^{13}\text{C}$  values from  $-7$  to  $-22$  per mil PDB, which suggests that organic carbon made significant contributions to the mineralizing fluids (Hoefs, 1973). The Gogo Formation is more organic rich than other units on the Lennard shelf (Alexander et al., 1985), and there can be little doubt that the anoxic muds that compacted to form black shales in that formation were the source of the carbon involved. The lack of extremely negative carbon isotopes (i.e.,  $\delta^{13}\text{C}$  values below  $-25$ ‰ PDB) in the deposits indicates that methane oxidation (Irwin et al., 1977; Schoell, 1988) did not have a dominant role in their development, as the  $\delta^{13}\text{C}$  values of stromatolites in the buildups are never below  $-22$  per mil PDB and are commonly significantly above that value (as high as  $-7$ ‰ PDB). However, it is possible that the lowest values represent some mixing of marine carbon with methane-derived carbon.

Iron and barium in the mineralizing fluids are thought to have been sourced from muds in the Gogo Formation. Compaction fluids derived from those horizons can be expected to have carried varying amounts of iron and barium in solution, depending on the concentrations of those elements in the source horizons and the prevailing chemical conditions.

#### Neomorphic alteration of stromatolites

Petrologic and field observations of the dark-colored fibrous calcite indicate that it is a recrystallization product of light-colored calcite. Two observations indicate that the sulfide-precipitating fluids were responsible for this recrystallization: the outcrop association between gossan veins and dark-colored (recrystallized) calcite (Fig. 7H); and the presence of microinclusions of pyrite in dark- but not in light-colored calcite.

The dark-colored (recrystallized) calcite has uniform stable isotope values, with very negative carbon and oxygen isotopes similar to those of primary marine cements (Fig. 10). This is in accord with the interpretation that fluids responsible for recrystallization were early diagenetic marine waters that had been involved in bacterial sulfate reduction and organic matter oxidation.

The trace element concentrations also reveal much about the nature of the fluids involved in forming the dark- and light-colored calcites. The matrix of the dark-colored calcite generally has lower iron values and higher manganese, strontium, and magnesium values than the light-colored calcite (Fig. 11). The low iron values and high ratios of manganese to iron are to be expected if the fluids that precipitated sulfides were also responsible for recrystallization; that is because a fluid remaining after iron sulfide precipitation would be depleted in iron but not in manganese. The high strontium and magnesium concentrations point to a marine-like fluid as being responsible for recrystallization (Veizer, 1983).

The occurrence, petrology, and geochemistry of the dark-colored calcites indicate that they were recrystallized during very early diagenesis by the same fluids that precipitated the iron sulfides. This recrystallization resulted in the destruction of many original fabrics. The light-colored calcites, on the other hand, have retained their primary fabrics, and their mineralogy was probably stabilized later, during deeper burial diagenesis, as indicated by their lower magnesium, strontium, and oxygen isotope values (Choquette and James, 1987). The higher  $\delta^{13}\text{C}$  values in the light-colored calcites indicate that their carbon was contributed from both marine and organic sources, and their fabric-retaining form suggests that the precursor mineral was high magnesium calcite, altered after burial to low magnesium calcite (James and Choquette, 1984).

#### Barite and iron sulfide precipitation

After precipitating iron sulfides in fissures and recrystallizing adjoining parts of the stromatolitic limestones, the fluids progressed to the upper surfaces of the buildups, where they nourished microbial communities and mixed with oxygenated seawater. Barium dissolved in the fluids was oxidized, precipitating barite, intergrown with stromatolites and filling fissures. Sulfur in the barite is extremely heavy ( $\delta^{34}\text{S}$  values ranging from 38–50‰ CDT), which is consistent with a residual sulfur source after extensive bacterial sulfate reduction in a closed system. It contrasts with marine barite described by previous authors (e.g., Cortecchi and Longinelli, 1972), which has similar values to that of seawater (about 20‰ CDT).

The precipitation of barite in the upper parts of the buildups indicates that water conditions on the sea floor were

TABLE 2. Sulfur Isotope Analyses for Surface Samples of Barite and Drill Core Samples of Iron Sulfides in Stromatolite-Barite-Sulfide Exhalative Deposits

Deposit	Sample no.	Mineral	$\delta^{34}\text{S}$ ‰ CDT
Longs Well	N 33	Barite	39.0
Longs Well	N 24	Barite	50.0
Minnie Pool	13501	Barite	37.8
Minnie Pool	13502	Barite	44.1
Longs Well <sup>1</sup>	T29-V7	Iron sulfide	35.9
Longs Well <sup>1</sup>	V4 15.5 m	Iron sulfide	35.3
Longs Well <sup>1</sup>	V4 22.6 m	Iron sulfide	36.2
Longs Well <sup>1</sup>	V10 136.5 m	Iron sulfide	36.3
Longs Well <sup>1</sup>	V10 185.2 m	Iron sulfide	32.9
Longs Well <sup>1</sup>	XD1 63.6 m	Iron sulfide	37.5

<sup>1</sup> Drill core samples, data from De Kever (1998) and Mason (1998)

relatively oxidized (i.e., more oxidized than at the sulfate-sulfide boundary). However, the lack of any marine benthic faunas, and the periodic precipitation of iron sulfide over stromatolites on the sea floor (Fig. 9C), suggests that oxygen levels were normally low. Most of the iron sulfide precipitation occurred in subsurface fissures, under anoxic conditions.

Iron sulfides within the buildups occur mainly as fissure fillings and to a lesser extent as other cavity fillings and replacements of micrite matrix. As is the case with barite, the high sulfur isotope values of the iron sulfides ( $\delta^{34}\text{S}$  values ranging from 33–37.5‰ CDT) are consistent with a source of residual sulfur after sulfate reduction in the Gogo Formation. The iron is also probably derived from the Gogo Formation, where it was present either as iron oxides or combined in clay minerals. It is possible that some of the early reduced sulfur was consumed in iron-bearing horizons within the Gogo Formation, through the precipitation of iron sulfides, and that the remaining sulfur was expelled in iron-free compaction fluids. The reduced sulfur in those fluids would then be transported until it encountered a new source of iron, probably contained in compaction fluids derived from other horizons in the Gogo Formation. Iron sulfide precipitation would then occur where reduced sulfur- and iron-bearing fluids were mixed in suitable environments, such as fissures within the buildups. Any remaining reduced sulfur would be oxidized in seawater at or near the tops of the buildups, resulting in barite precipitation, as previously described.

#### *Epigenetic Zn-Pb sulfides*

The only epigenetic sulfide mineralization that has been found within the stromatolite-barite-sulfide deposits are minor veins of zinc, lead, and iron sulfides, not more than a few centimeters wide, that crosscut and replace the earlier exhalative iron sulfides (Fig. 6).

The economic Zn-Pb deposits on the Lennard shelf exhibit features that are characteristic of late-stage epigenetic deposits. They are controlled by faults and joints that acted as pathways for hydrothermal mineralizing fluids. Those fluids dissolved carbonates, forming cavity systems in which the sulfides were precipitated. Some mineralization is also interpreted to have replaced Devonian carbonates and evaporites (Tompkins et al., 1994b; Vearncombe et al., 1995). Unlike the exhalative sulfides, the epigenetic Zn-Pb sulfides postdate marine cements, regional dolomitization, and the onset of stylolitization.

The main reasons for the lack of Zn and Pb sulfides contemporaneous with the exhalative buildups are probably that the fluids involved were too cold and not saline enough to carry significant amounts of zinc and lead. High concentrations of chloride (>100,000 mg/l) seem to be necessary before substantial quantities of those metals can be transported in solution and their solubility rises steeply with increased temperature (Hanor, 1996). The epigenetic deposits are believed to have formed from relatively high temperature brines derived from the Fitzroy trough (Arne, 1996), whereas the exhalative fluids responsible for the Devonian buildups are thought to have had salinities resembling that of normal seawater, and with temperatures that were less than 60°C and probably less than 40°C. However, iron and barium can be carried readily in such cool fluids (Barnaby and Rimstidt, 1989; Garrels and Christ, 1990).

The epigenetic and syngenetic (exhalative) types of mineralization on the Lennard shelf were both probably sourced in basinal shales, from which the mineralizing fluids were driven by compaction. Such compaction must have commenced immediately after deposition of muds in the Gogo Formation and continued for many millions of years during the remainder of the Late Devonian and early Carboniferous.

In the case of the epigenetic Zn-Pb deposits on the Lennard shelf (principally Pillara, Cadjebut, and Goongewa, Fig. 1), the mineralizing system was on a larger scale, and the fluids are thought to have originated during the latest Devonian or early Carboniferous, through the deep-burial diagenesis of shales at a time when the adjoining Fitzroy trough was subject to strong subsidence and extension. Hot (up to about 90°C) zinc-, lead-, and iron-bearing brines were probably derived from thick Devonian shales in the Fitzroy trough. The expelled fluids were channeled along faults into carbonates of the Devonian reef complexes on the adjoining Lennard shelf, where Zn-Pb sulfides were precipitated in fractured carbonates, hydrothermal karst cavities, and evaporitic beds (Vearncombe et al., 1995).

One of the principal questions remaining is whether or not significant sea-floor exhalation of fluids continued during the long time interval between deposition of the stromatolite-barite-sulfide deposits and that of the epigenetic sulfides. Perhaps fluid expulsion was a steady process linked with the progressive compaction of shales throughout the Late Devonian and early Carboniferous. Alternatively, major expulsion of fluids may have been episodic, associated with rapid compaction during periods of strong tectonism. In that case there might have been only two significant periods of mineralization: syngenetic (exhalative) mineralization in the Frasnian (Late Devonian), and epigenetic (Mississippi Valley-type) mineralization in the late Famennian (latest Devonian) or early Carboniferous.

#### **Comparisons to Other Seep and Vent Systems**

The stromatolite-barite-sulfide deposits described here have some different characteristics from those of other buildups known to have developed over cold-seep and hot-vent systems in modern and ancient environments. Numerous examples of modern and ancient carbonate buildups related to hydrocarbon seeps have been documented (e.g., Beauchamp and Savard, 1992; Hovland, 1992; Carney, 1994; Aharon et al., 1997). However, there is no evidence of hydrocarbons being associated with the Devonian exhalative buildups of the Lennard shelf. Moreover, whereas well-developed benthic faunas (forming oases surrounded by deserts) are known to be intimately associated with modern exhalative buildups, no such faunas were developed on the Devonian buildups.

In most modern and ancient exhalative systems, extremely negative carbon isotope values in the associated carbonates and pore fluids (having  $\delta^{13}\text{C}$  values less than -25‰ PDB) point to the influence of biogenic or abiogenic methane (e.g., von Rad et al., 1996; Cavagna et al., 1999; Stakes et al., 1999). High methane concentrations have also been measured from bottom waters sampled around modern sea-floor seeps (e.g., Kulm et al., 1986; Boulegue et al., 1987). Although methane can be expected to have been one of the gases exhaled during

early compaction of shales in the Gogo Formation, there is no isotopic evidence to show that it was a major source of the associated carbonates. Instead, the evidence points to bacterial oxidation of organic matter rather than methanogenesis as the principal source of those carbonates.

Texturally, the Lennard shelf buildups are unusual in having been constructed mainly by fibrous calcite. Other known cool-seep carbonates, both modern and ancient, consist predominantly of micrite (e.g., von Rad et al., 1996; Belka, 1998; Stakes et al., 1999), although fibrous stromatolitic calcites are known from nonmarine deposits, including tufa (Freytet and Verrecchia, 1999) and hot travertine (Chafetz and Guidry, 1999).

### Conclusions

1. Stromatolite-barite-sulfide deposits in Devonian reef complexes of the Canning basin are interpreted to be exhalative deposits, formed as low mounds above cool-fluid seepages on the sea floor.

2. The exhalative interpretation is based on the following observations and interpretations: (1) major compaction of basinal shales in the Gogo Formation, beginning soon after deposition, must have resulted in the expulsion of large volumes of interstitial fluids; (2) the in situ deposits are lenticular stromatolitic buildups localized over features that could be expected to have acted as pathways for compaction-driven fluids—synsedimentary faults and contacts between shales of the Gogo Formation and marginal-slope limestones of the Sadler Limestone; (3) isotopic and petrographic evidence suggests that early diagenetic reactions in shales of the Gogo Formation, involving bacterial sulfate reduction and bacterial oxidation of organic matter, were important in forming the mineralizing fluids; and (4) the syngenetic origin of the mineralization is shown by the occurrence in penecontemporaneous debris-flow deposits of blocks derived from stromatolite-barite-sulfide buildups and by evidence that some sulfide deposition occurred over stromatolite columns on the sea floor.

3. Chemosynthetic bacteria, nourished by cool-water seepages, are likely to have played significant roles in precipitating stromatolites, barite, iron sulfides, and concretions, although inorganic precipitation may also have been involved.

4. Sedimentary veins of iron sulfides (pyrite and marcasite), now weathered to limonitic gossans, filled early fissures in the stromatolite buildups and may have been precipitated by the mixing of sulfur- and iron-bearing compaction-driven fluids.

5. The mineralizing fluids permeated and recrystallized adjoining parts of the stromatolite buildups and were oxidized on encountering seawater at the upper surfaces of the buildups, resulting in the precipitation of barite intergrown with stromatolites and filling small veins.

6. Syngenetic mineralization in the exhalative buildups is of no economic value, but at least one buildup is cut by minor veins of epigenetic Zn-Pb mineralization, and important epigenetic Zn-Pb deposits, formed many millions of years after growth of the buildups, have been mined in the same general area of the basin.

7. The epigenetic phase of mineralization, like the earlier exhalative phase, is interpreted to have resulted from dewatering

of basinal shales, but it is unsure whether the two phases represent end members of a continuing process that involved steady rates of shale compaction, fluid expulsion, and sulfide precipitation or were episodic, resulting from major pulses of tectonism.

### Acknowledgments

We wish to thank Roger Hocking and Iain Copp of the Geological Survey of Western Australia for their assistance in the field, and Nicole De Kever and Rebecca Mason of the University of Melbourne for their contributions to knowledge of the Longs Well and East Pillara areas. Thanks are also due David Groves, Franco Pirajno, and Ian Tyler for advice and suggestions, reviewers Ross Large and Ross Both for comments, corrections, and suggestions, Marco Einaudi for editorial advice, and Western Metals N.L. and BHP Minerals Ltd for facilitating our research in a number of ways. This paper is published with the permission of the Director, Geological Survey of Western Australia.

November 15, 2000; June 13, 2001

### REFERENCES

- Aharon, P., Schwarcz, H.P. and Roberts, H.H., 1997, Radiometric dating of submarine hydrocarbon seeps in the Gulf of Mexico: Geological Society of America Bulletin, v. 109, p. 568–579.
- Alexander, R., Cumbers, K.M., Hartung, B., and Kagi, R.I., 1985, Petroleum geochemistry of the Canning basin: Perth, WA, Western Australian Mining and Petroleum Research Institute Report 20, 119 p.
- Arne, D., 1996, Thermal setting of the Cadjebut Zn-Pb deposit, Western Australia: Journal of Geochemical Exploration, v. 57, p. 45–56.
- Banks, D.A., 1985, A fossil hydrothermal worm assemblage from the Tynagh lead-zinc deposit in Ireland: Nature, v. 313, p. 128–131.
- Barnaby, R.J., and Rimstidt, J.D., 1989, Redox conditions of calcite cementation interpreted from Mn and Fe contents of authigenic calcites: Geological Society of America Bulletin, v. 101, p. 795–804.
- Beauchamp, B., and Savard, M., 1992, Cretaceous chemosynthetic carbonate mounds in the Canadian Arctic: Palaios, v. 7, p. 434–450.
- Belka, Z., 1998, Early Devonian Kess-Kess carbonate mud mounds of the eastern Anti-Atlas (Morocco), and their relation to submarine hydrothermal venting: Journal of Sedimentary Research, v. 68, p. 368–377.
- Bennett, M.R.C., 1992, Reports on drilling programme, Virgin Hills (EL 04/610), April 1991-June 1992: Geopeko unpublished reports WA92/22S, WA93/610, Geological Survey of Western Australia Open-File Reports A35758, A57568.
- 1994, Final report for Virgin Hills E 04/610 for the period May 1992 to July 1993: Geopeko unpublished report WA 94/46S, Geological Survey of Western Australia Open-File Report A39973.
- Boulegue J., Iiyama, J.T, Charlou, J., and Jedwab, J., 1987, Nankai trough, Japan trench and Kuril trench: Geochemistry of fluids sampled by submersible "Nautile": Earth and Planetary Science Letters, v. 83, p. 363–375.
- Boyce, A.J., Coleman, M.L., and Russell, M.J., 1983, Formation of fossil hydrothermal chimneys and mounds from Silvermines, Ireland: Nature, v. 306, p. 545–550.
- Brannon, J.C., Cole, S.C., Podosek, F.A., Ragan, V.M., Coveney, R.M., Jr., Wallace, M.W., and Bradley, A.J., 1996, Th-Pb and U-Pb dating of ore-stage calcite and Paleozoic fluid flow: Science, v. 271, p. 491–493.
- Broadbent, G.C., Myers, R.E., and Wright, J.V., 1998, Geology and origin of shale-hosted Zn-Pb-Ag mineralization at the Century deposit, northwest Queensland, Australia: ECONOMIC GEOLOGY, v. 93, p. 1264–1294.
- Carney, R.S., 1994, Consideration of the oasis analogy for chemosynthetic communities at Gulf of Mexico hydrocarbon vents: Geo-Marine Letters, v. 14, p. 149–159.
- Cavagna, S., Clari, P., and Martire, L., 1999, The role of bacteria in the formation of cold seep carbonates: Geological evidence from Monferrato (Tertiary, NW Italy): Sedimentary Geology, v. 126, p. 253–270.
- Chafetz, H.S., and Guidry, S.A., 1999, Bacterial shrubs, crystal shrubs, and ray-crystal shrubs: Bacterial vs. abiotic precipitation: Sedimentary Geology, v. 126, p. 57–74.

- Choquette, P.W., and James, N.P., 1987, Diagenesis in limestones. 3. The deep burial environment: *Geoscience Canada*, v. 14, p. 3–35.
- Christensen, J.N., Halliday, A.N., Vearncombe, J.R. and Kesler, S.E., 1995, Testing models of large-scale crustal fluid flow using direct dating of sulfides: Rb-Sr evidence for early dewatering and formation of Mississippi Valley-type deposits, Canning basin, Australia: *ECONOMIC GEOLOGY*, v. 90, p. 877–884.
- Church, T.M., 1979, Marine barite, origin and occurrence: *Reviews in Mineralogy*, v. 6, p. 175–209.
- Claypool, G.E., Holster, W.T., Kaplan, I.R., Sakai, H., and Zak, I., 1980, The age curves of sulfur and oxygen isotopes in marine sulfate and their mutual interpretation: *Chemical Geology*, v. 28, p. 199–260.
- Cooke, D.R. Bull, S.W. Large, R.R. and McGoldrick, P.J., 2000, The importance of oxidized brines for the formation of Australian Proterozoic stratiform sediment-hosted Pb-Zn (sedex) deposits: *ECONOMIC GEOLOGY*, v. 95, p. 1–17.
- Copp, I.A., 2000, Subsurface facies analysis of Devonian reef complexes, Lennard shelf, Canning basin, Western Australia: *Geological Survey of Western Australia Report 58*, 127 p.
- Cortecci, G., and Longinelli, A., 1972, Oxygen isotope variations in a barite slab from the sea bottom off California: *Chemical Geology*, v. 9, p. 113–117.
- Curtis, C.D., Oertel, G., and Petrowski, C., 1972, Stable carbon isotope ratios within carbonate concretions: A clue to place and time of formation: *Nature*, v. 235, p. 98–100.
- De Kever, N., 1998, Devonian stromatolites and exhalative mineralization, Canning basin, Western Australia: Unpublished B.Sc. (Honors) thesis, Parkville, Victoria, School of Earth Sciences, University of Melbourne, 144 p.
- Dörling, S.L., Dentith, M.C., and Playford, P.E., 1995, Deformation in the carbonate rocks of the Lennard shelf: *Society of Economic Geologists Guidebook Series*, v. 23, p. 51–80.
- Fleming, B.S., 1983, Lennard shelf regional Pb-Zn exploration, Lawford Range E.L. 80/116 (formerly Emanuel Range Prospect), West Kimberley and Kimberley mineral fields, Western Australia: BHP Minerals Limited unpublished report, Geological Survey of Western Australia Open-File Report A14063.
- Freytet, P., and Verrecchia, E.P., 1999, Calcitic radial palisade fabric in freshwater stromatolites: Diagenetic and recrystallized feature or physico-chemical sinter crust: *Sedimentary Geology*, v. 126, p. 97–102.
- Garrels, R.M., and Christ, C.L., 1990, *Solutions, minerals and equilibria*: Boston, Jones and Bartlett, 450 p.
- Goldberg, E.D., and Arrhenius, G.O.S., 1958, Chemistry of Pacific pelagic sediments: *Geochimica et Cosmochimica Acta*, v. 13, p. 153–212.
- Goldstein, R.H., and Reynolds, T.J., 1994, Systematics of fluid inclusions in diagenetic minerals: *Society of Economic Paleontologists and Mineralogists Short Course 31*, 199 p.
- Hanor, J.S., 1996, Controls on the solubilization of lead and zinc in basinal brines: *Society of Economic Geologists Special Publication 4*, p. 483–500.
- Hitzman, M.W., and Beaty, D.W., 1997, The Irish Zn-Pb-(Ba) orefield: *Society of Economic Geologists Special Publication 4*, p. 112–143.
- Hocking, R.M., Copp, I.A., Playford, P.E., and Kempton, R.H., 1996, The Cadjebut Formation: A Givetian evaporitic precursor to Devonian reef complexes of the Lennard shelf, Canning basin, Western Australia: *Geological Survey of Western Australia Annual Review 1995-96*, p. 48–55.
- Hoefs, J., 1973, *Stable isotope geochemistry*: New York, Springer-Verlag, 140 p.
- Hovland, M., 1992, Hydrocarbon seeps in northern marine waters—their occurrence and effects: *Palaeos*, v. 7, p. 376–382.
- Irwin, H., Curtis, C., and Coleman, M., 1977, Isotopic evidence for source of diagenetic carbonates formed during burial of organic-rich sediments: *Nature*, v. 269, p. 209–213.
- James, N.P., and Choquette, P.W., 1984, Diagenesis. 6. Limestones, the sea floor diagenetic environment: *Geoscience Canada*, v. 10, p. 162–179.
- Kaiser, C.J., Kelly, W.C., Wagner, R.J., and Shanks, W.C., III, 1987, Geologic and geochemical controls of mineralization in the Southeast Missouri barite district: *ECONOMIC GEOLOGY*, v. 82, p. 719–734.
- Kerans, C., 1985, Petrology of Devonian and Carboniferous carbonates of the Canning and Bonaparte basins: Perth, WA, Western Australian Mining and Petroleum Research Institute Report 12, 203 p.
- Kulm, L.V.D., Suess, E., Moore, J.C., Carson, B., Lewis, B.T., Ritger, S.D., Kadko, D.C., Thornburg, T.M., Embley, R.W., Rugh, W.D., Massoth, G.J., Langseth, M.G., Cochrane, G.R., and Scamman, R.L., 1986, Oregon subduction zone: Venting, fauna, and carbonates: *Science*, v. 231, p. 561–566.
- Large, R.R., Bull, S.W., Cooke, D.R., and McGoldrick, P.J., 1998, A genetic model for the HYC deposit, Australia: Based on regional sedimentology, geochemistry, and sulfide-sediment relationships: *ECONOMIC GEOLOGY*, v. 93, p. 1345–1368.
- Mason, R., 1998, Exhalative carbonate mineralization of the East Pillara Range, Lennard shelf, Western Australia: Unpublished B.Sc. (Honors) thesis, Parkville, Victoria, School of Earth Sciences, University of Melbourne, 70 p.
- Masuzawa, T., Handa, N., Kitagawa, H., and Kusakabe, M., 1992, Sulfate reduction using methane in sediments beneath a bathyal “cold seep” giant clam community off Hatsushima Island, Sagami Bay, Japan: *Earth and Planetary Science Letters*, v. 110, p. 39–50.
- McManus, A., and Wallace, M.W., 1992, Age of Mississippi Valley-type sulfides determined using cathodoluminescence cement stratigraphy, Lennard shelf, Canning basin, Western Australia: *ECONOMIC GEOLOGY*, v. 87, p. 189–193.
- Murphy, G.C., 1990, Lennard shelf lead-zinc deposits, in Hughes, F.E., ed., *Geology of the mineral deposits in Australia and Papua New Guinea*: Melbourne, Australasian Institute of Mining and Metallurgy, p. 1103–1109.
- Paytan, A., Kastner, M., and Martin, E.E., 1993, Marine barite as a monitor of seawater strontium isotope composition: *Nature*, v. 366, p. 445–449.
- Peace, W.M., and Wallace, M.W., 2000, Timing of mineralization at the Navan Zn-Pb deposit: A post-Arundian age for Irish mineralization: *Geology*, v. 28, p. 711–714.
- Perkins, W.G., and Bell, T.H., 1998, Stratiform replacement lead-zinc deposits: A comparison between Mount Isa, Hilton and McArthur River: *ECONOMIC GEOLOGY*, v. 93, p. 1190–1212.
- Playford, P.E., 1980, Devonian “Great Barrier reef” of Canning basin, Western Australia: *American Association of Petroleum Geologists Bulletin*, v. 64, p. 814–840.
- 1999, Devonian stromatolites and exhalative mineralization, Canning basin, Western Australia: *Geological Survey of Western Australia Record 1999/6*, p. 14–15.
- Playford, P.E., and Cockbain, A.E., 1992, Devonian reef complexes of the Canning basin, Western Australia: *Petroleum Exploration Association of Australia and American Association of Petroleum Geologists Field Trip Guidebook 1*, 161 p.
- Playford, P.E., and Hocking, R.M., 1999, Devonian reef complexes of the Canning basin: *Geological Survey of Western Australia Geological Maps of the Lennard shelf (Preprints of plates 1-7 to accompany Bulletin 145)*.
- Playford, P.E., and Wallace M.W., 1998, Stromatolites and sedimentary-exhalative mineralization in the Devonian of the Canning basin, Western Australia [abs.]: *Geological Society of Australia, Australian Geological Convention, 14<sup>th</sup>, Townsville, Queensland, 1998, Abstracts 49*, p. 357.
- Playford, P.E., Cockbain, A.E., Druce, E.C., and Wray, J.L., 1976, Devonian stromatolites from the Canning basin, Western Australia, in Walter, M.R., ed., *Stromatolites*: Amsterdam, Elsevier, p. 543–564.
- Playford, P.E., Wallace, M.W., De Kever, N., and Mason, R., 1999, Devonian stromatolites and exhalative mineralization, Canning basin, Western Australia [abs.]: *American Association of Petroleum Geologists Annual Meeting, San Antonio, Texas, 1999, Abstracts*, p. A 110.
- Riding, R., 2000, Microbial carbonates: The geological record of calcified bacterial-algal mats and biofilms: *Sedimentology*, v. 47, p. 179–214.
- Ringrose, C.R., 1989, Studies of selected carbonate-hosted lead-zinc deposits in the Kimberley region: *Geological Survey of Western Australia Report 24*, 103 p.
- Russell, M.J., 1996, The generation at hot springs of sedimentary ore deposits, microbialites and life: *Ore Geology Reviews*, v. 10, p. 199–214.
- Schoell, M., 1988, Multiple origins of methane in the earth: *Chemical Geology*, v. 71, p. 1–10.
- Shearley, E., Redmond, P., King, M., and Goodman, R., 1996, Geological controls on mineralisation and dolomitisation of the Lisheen Zn-Pb-Ag deposit, Co. Tipperary, Ireland: in Strogon, P., Somerville, I.D., and Jones, G.L., eds., *Recent advances in Lower Carboniferous geology*: Dublin, Geological Society Special Publication, p. 23–33.
- Stakes, D.S., Orange, D.L., Paduan, J.B., Salamy, K.A., and Maher, N., 1999, Cold-seeps and authigenic carbonate formation in Monterey Bay, California: *Marine Geology*, v. 159, p. 93–109.
- Tompkins, L.A., Pedone, V.A., Roche, M.T., and Groves, D.I., 1994a, The Cadjebut deposit as an example of Mississippi Valley-type mineralization on the Lennard shelf, Western Australia: Single episode or multiple events?: *ECONOMIC GEOLOGY*, v. 89, p. 450–466.

- Tompkins, L.A., Rayner, M.J., Groves, D.I., and Roche, M.T., 1994b, Evaporites: In situ sulfur source for rhythmically banded ore in the Cadjebut Mississippi Valley type Zn-Pb deposit, Western Australia: *ECONOMIC GEOLOGY*, v. 89, p. 467-492.
- Torres, M.E., Bohrmann, G., and Suess, E., 1996, Authigenic barites and fluxes of barium associated with fluid seeps in the Peru subduction zone: *Earth and Planetary Science Letters*, v. 144, p. 469-481.
- Tucker, R.D., Bradley, D.C., Ver Straeten, C.A., Harris, A.G., Ebert, J.R., and McCutcheon, S.R., 1998, New U-Pb zircon ages and the duration and division of Devonian time: *Earth and Planetary Science Letters*, v. 158, p. 175-186.
- Vearncombe, J.R., Dörling, S.L., Dentith, M.C., Chisnall, A.W., Christensen, J.N., McNaughton, N.J., Playford, P.E., Rayner, M.J., and Reed, A.R., 1995, Zinc-lead mineralization on the southeastern Lennard shelf, Canning basin, Western Australia: *Society of Economic Geologists Guidebook Series*, v. 23, 218 p.
- Veizer, J., 1983, Chemical diagenesis of carbonates: Theory and application of trace element technique: *Society of Economic Paleontologists and Mineralogists Short Course 10*, p. 3-1 to 3-100.
- von Rad, U., Roesch, H., Berner, U., Geyh, M., Marchig, V., and Schulz, H., 1996, Authigenic carbonates derived from oxidized methane vented from the Makran accretionary prism off Pakistan: *Marine Geology*, v. 136, p. 55-77.
- Wallace, M.R., Kerans, C., Playford, P.E., and McManus, A., 1991, Burial diagenesis in the Upper Devonian reef complexes of the Geikie Gorge region, Canning basin, Western Australia: *American Association of Petroleum Geologists Bulletin*, v. 75, p. 1018-1038.
- Walter, M.R., 1976, Stromatolites: *Developments in Sedimentology* 20, 790 p.
- Young, G.C. and Laurie, J.R., *An Australian Phanerozoic timescale*: Melbourne, Oxford University Press, 279 p.